Steel and Composite Structures, Vol. 11, No. 6 (2011) 505-524
DOI: http://dx.doi.org/10.12989/scs.2011.11.6.505

Linear buckling analysis of welded girder webs with variable thickness

Emanuele Maiorana and Carlo Pellegrino*

Department of Structural and Transportation Engineering, University of Padova, Via Marzolo, 9, 35131 Padova, Italy

(Received December 22, 2009, Revised November 27, 2010, Accepted October 12, 2011)

Abstract. Steel girder web panels have been subjected in recent decades, to a number of experimental and numerical studies but the mechanisms that regulate the behaviour of the panels composed by two subpanels with different thickness were not deeply studied. Furthermore specific design rules regarding the estimation of the buckling coefficient for panels with variable thickness are not included in the codes even if this is a common situation particularly for steel bridge girders with beams having significant height. In this framework, this work aims to investigate buckling behaviour of steel beams with webs composed of panels with different thicknesses subjected to both in-plane axial compression and bending moment and gives some simplified equations for the estimation of the buckling coefficient.

Keywords: stability; steel panel; linear buckling; design.

1. Introduction

Thin plates are commonly used in a number of steel structures, traditionally in shipping and aircraft, but also heavily in significant civil infrastructure like bridges, viaducts and offshore structures.

In the last decades web panels of bridge beams have been the subject of a number of experimental and numerical studies. The analytical closed-form solution to determine the elastic critical load (Timoshenko and Woinowsky-Krieger 1959) was obtained in simple cases (e.g. uniform compression in panels with constant thickness), whereas solutions derived from experimental and numerical investigations have been used for other load conditions and geometries. In particular the use of Finite Element (FE) method allowed the study of any geometry, initial imperfections (Sadovský *et al*. 2005, Maiorana *et al*. 2009a), particular configurations of the load as patch loading (Maryland *et al*. 1999, Granath and Lagerqvist 1999), and a wide range of constitutive laws for the material in linear and non-linear range (El-Sawy *et al*. 2004, Ren and Tong 2005, Alinia and Dastfan 2006, El-Sawy and Martini 2007, Paik 2007, Maiorana *et al*. 2008a, 2009b). A number of studies were devoted to the position of the stiffeners (Lee *et al*. 2002, Xie and Chapman 2004, Alinia 2005, Graciano and Casanova 2005, Pavlovčciè *et al*. 2007, Maiorana *et al*. 2011a) and perforated panels (Cheng and Fan 2001, Lian and Shanmugam 2003, Azhari *et al*. 2005, Komur and Sonmez 2008, Maiorana *et al*. 2008b, Yang *et al*. 2008, Maiorana *et al*. 2009c, 2011b, Pellegrino *et al*. 2009).

* Corresponding author, Ph. D., E-mail: carlo.pellegrino@unipd.it

The codes for design of steel panels, in particular the Eurocode (EN 1993–1–5 2007), usually consider some simple configurations that often underestimate the real potentialities of the panels related to the elastic critical load and ultimate strength.

Covering large spans in bridge construction often imply the use of web panels having significant height in beams consisting of at least two plates with different thicknesses. The mechanisms governing the behaviour of the panels composed by two subpanels with different thickness were not deeply studied and the relative design rules are not explicitly included in the codes (Chatterjee 2003). In this framework, this work aims to investigate buckling behaviour of steel beams with webs composed of panels with different thicknesses subjected to both in-plane axial compression and bending moment and give some simplified equations for the estimation of the buckling coefficient.

2. Methodology

Linear buckling analysis leads to the determination of the elastic critical load through the resolution of the eigenvalue problem. The lower eigenvalue corresponds to the elastic critical load whereas the eigenvector defines the corresponding deformed shape. Buckling load of simply supported plates subjected to uniform compression and constant thickness is analytically determined by solving the well known Eq. (1). The meaning of the symbols is shown in appendix.

$$D\nabla^4\omega + \bar{N}_x\frac{\partial^2\omega}{\partial \mathrm{x}^2} = 0 \tag{1}$$

with the following boundary conditions

$$\omega = 0 \quad \frac{\partial^2\omega}{\partial x^2} = 0 \quad \text{along } x = 0;a$$

$$\omega = 0 \quad \frac{\partial^2\omega}{\partial y^2} = 0 \quad \text{along } x = 0;h$$

The solution has the following form

$$\omega = \sum_{m=1}^{\infty}\sum_{n=1}^{\infty} A_{mn} sin\frac{m\pi\pi}{a} sin\frac{n\pi\pi}{h} \tag{2}$$

where m and n are integers that indicate the number of half-waves in x and y directions.
Substituting Eq. (2) into Eq. (1) one obtains

$$A_{mn}\left[\pi^4\left(\frac{m^2}{a^2}+\frac{n^2}{h^2}\right)-\frac{\bar{N}_x}{D}\frac{m^2\pi^2}{a^2}\right] = 0 \tag{3}$$

Therefore

$$\bar{N}_x = \frac{\pi^2 D}{h^2}\left(m\frac{h}{a}+\frac{n^2}{m}\frac{a}{n}\right)^2 \tag{4}$$

The lower value of $\bar{N}_x$ is obtained with $n = 1$ and instability occurs with the single half-wave in y direction for the value

$$\bar{N}_{xC} = \frac{k\pi^2 D}{h^2} \tag{5}$$

or, in term of stress

$$\sigma_{xC} = \frac{\bar{N}_{xC}}{t} = k\frac{\pi^2 E}{12(1-\nu^2)}\frac{1}{(h/t)^2} \tag{6}$$

where the buckling coefficient k is

$$k = \left(m\frac{h}{a} + \frac{1}{m}\frac{a}{h}\right)^2 \tag{7}$$

For uniformly loaded plate, with $a/h = 2$, $m = 2$ and $k = 4$. Other details could be found in (Timoshenko and Woinowsky-Krieger 1959).

From Eq. (7) it follows that, for plates with constant thickness, k does not depend on the panel slenderness λ.

For web panels composed by two longitudinally welded subpanels with different thicknesses (t' and t'') and heights (h' and h''), the influence of the slenderness of the single subpanel on the adjacent one cannot be neglected. In this context, the shape of the critical deformed configuration of the panel has to be observed to obtain some information.

It is assumed that plate behaviour is linearly elastic and the critical stress is less than that corresponding to the yield strength of the material. Straus7 code ver. 2.3.3 (G + D Computing 2005) was used for the analyses shown in this work.

A pilot study was conducted on a rectangular plate with $a/h = 2$ and constant thickness subjected to uniform compressive load for which the analytical buckling coefficient is $k = 4$. A comparison between deformed shapes for various geometric configurations, changing both height and thickness ratios, was developed maintaining uniform compressive load. Fig. 1 shows the typical geometry of the plate, boundary conditions and loading configuration for uniform compression. The thickness of the bottom sub-plate having thickness t' was kept constant in all geometric configurations.

Fig. 2 shows, as an example, the critical deformed configuration of the rectangular plate with $a/h = 2$

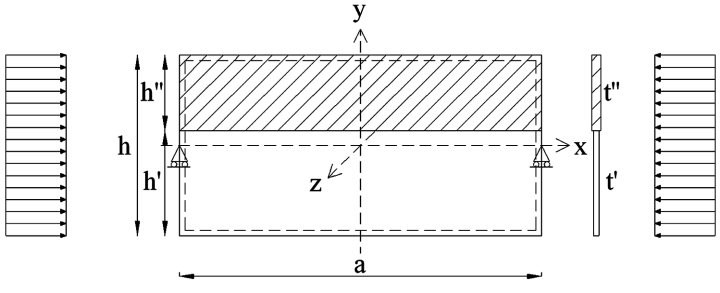

Fig. 1 Static scheme of the typical geometry of a plate with variable thickness

and $h''/h = 0.5$ subjected to uniform compressive load, for $t''/t' = 0.25$ (Fig. 2(a)), $t''/t' = 1$ (Fig. 2(b)) and $t''/t' = 3$ (Fig. 2(c)).

A significant difference between the thicknesses of the subpanels involves a buckling deformed configuration significantly different from the case of constant thickness since the number of half-waves

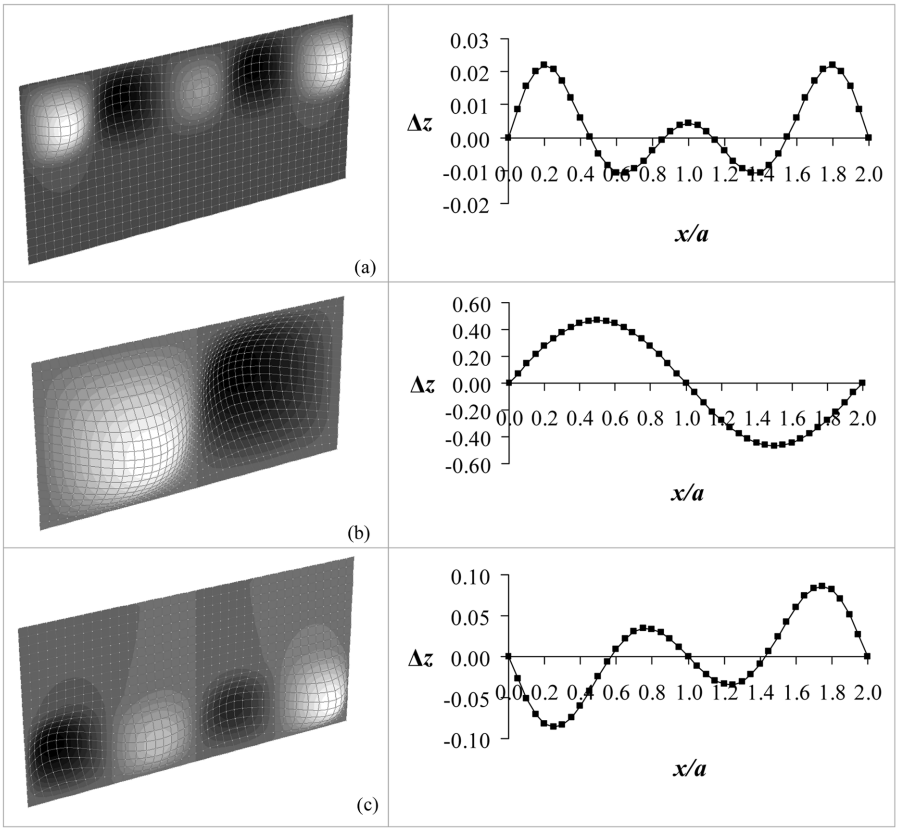

Fig. 2 Deformed shape for plates with $a/h = 2$ and $h''/h = 0.5$ subjected to uniform compressive load with $t''/t = 0.25$ (a); 1 (b) and 3 (c).

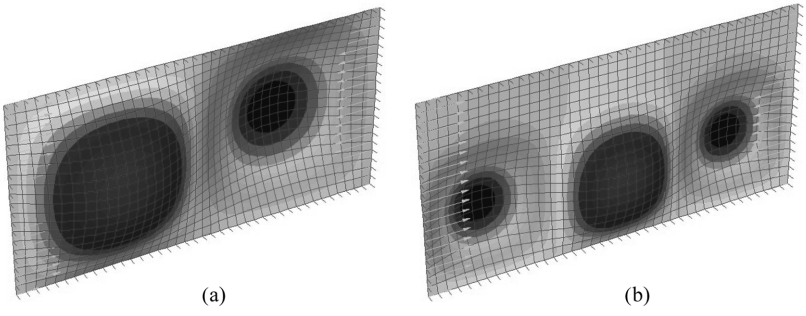

Fig. 3 Difference between the deformed shapes of a panel with constant thickness (left) and variable thickness (right). Plates with $a/h = 2$, $\psi = 1$, $h''/h = 0.25$, $t''/t' = 1$ (a) and $t''/t' = 3$ (b).

is also influenced by the ratio of the thicknesses of the two subpanels. In Fig. 3, as an example, the difference between the deformed shapes of a panel with constant thickness and variable thickness is shown. Plates with $a/h = 2$, $\psi = 1$, $h''/h = 0.25$, $t''/t' = 1$ (Fig. 3(a)) and $t''/t' = 3$ (Fig. 3(b)) were considered.

According to these preliminary results a systematic numerical study on linear buckling behaviour of square and rectangular plates with various h''/h and t''/t' ratios ($h''/h = 0.25, 0.5, 0.75$; $t''/t' = 0.25, 0.5, 0.75, 1, 1.25, 1.5, 2, 3$) was developed with the aim of giving some design equations for these geometric configurations with pure bending (with stress ratio $\psi = -1$), compression and bending with $\psi = -0.5$, 0 and 0.5, and uniform compression ($\psi = 1$). Fig. 4 shows the loading configurations considered in this study.

A sensitivity study on the mesh was preliminarily developed. The potential use of rectangular 4-nodes plate elements with six degrees of freedom for each node and triangular 3-nodes elements with six degrees of freedom for each node was investigated. A progressive refinement of the mesh was performed to obtain the discretization allowing sufficiently accurate results, without involving excessive computational effort. The following elements were considered: rectangular 4-nodes plate elements with regular dimensions $h/2$, $h/10$, $h/20$, $h/40$ and $h/80$; triangular 3-nodes elements with regular dimensions $h/2$, $h/10$, $h/20$ and $h/40$.

The buckling coefficient k does not significantly vary with the shape of the elements and the results do not show significant changes when further size reductions of 4-nodes plate elements occur from

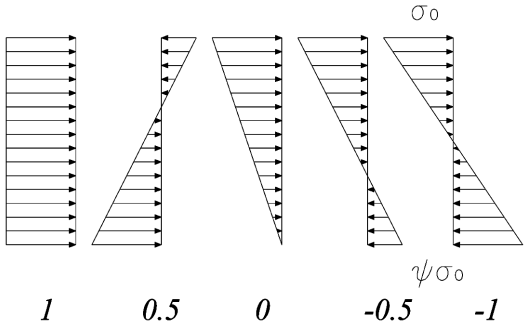

Fig. 4 Loading conditions for the typical plate

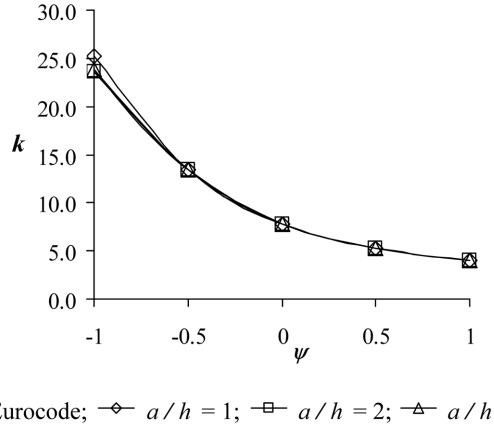

Fig. 5 Comparison of k values obtained with FE model and Eurocode equations for square and rectangular panels with constant thickness subjected to axial force and bending moment.

elements' dimensions equal to $h / 20$; hence this dimension was adopted.

Regarding the boundary conditions assumed in the analyses, the displacements in the out-of-plane direction are restrained along the edges of the plate whereas the rotations around the edges are free as shown in Fig. 1. The external load was directly applied to the nodes of the discretization with linearly variable trend along the height of the plate.

The FE-model was validated comparing, for square and rectangular plates with constant thickness, the buckling coefficient obtained with the FE model and corresponding Eurocode predictions (EN 1993–1–5 2007) for the load conditions considered in this study. The results of the FE model well fit Eurocode provisions for each plate and load condition (see Fig. 5).

3. Square plates

In this section, the behaviour in terms of global buckling coefficient k of square plates formed by two subpanels (see Fig. 1) subjected to various stress ratios ψ (see Fig. 4) is shown and discussed when h'' / h and t'' / t' vary. For plates with $a / h = 1$, Fig. 6 shows the k vs. ψ diagrams for $t'' / t' = 0.25$ (Fig. 6(a)),

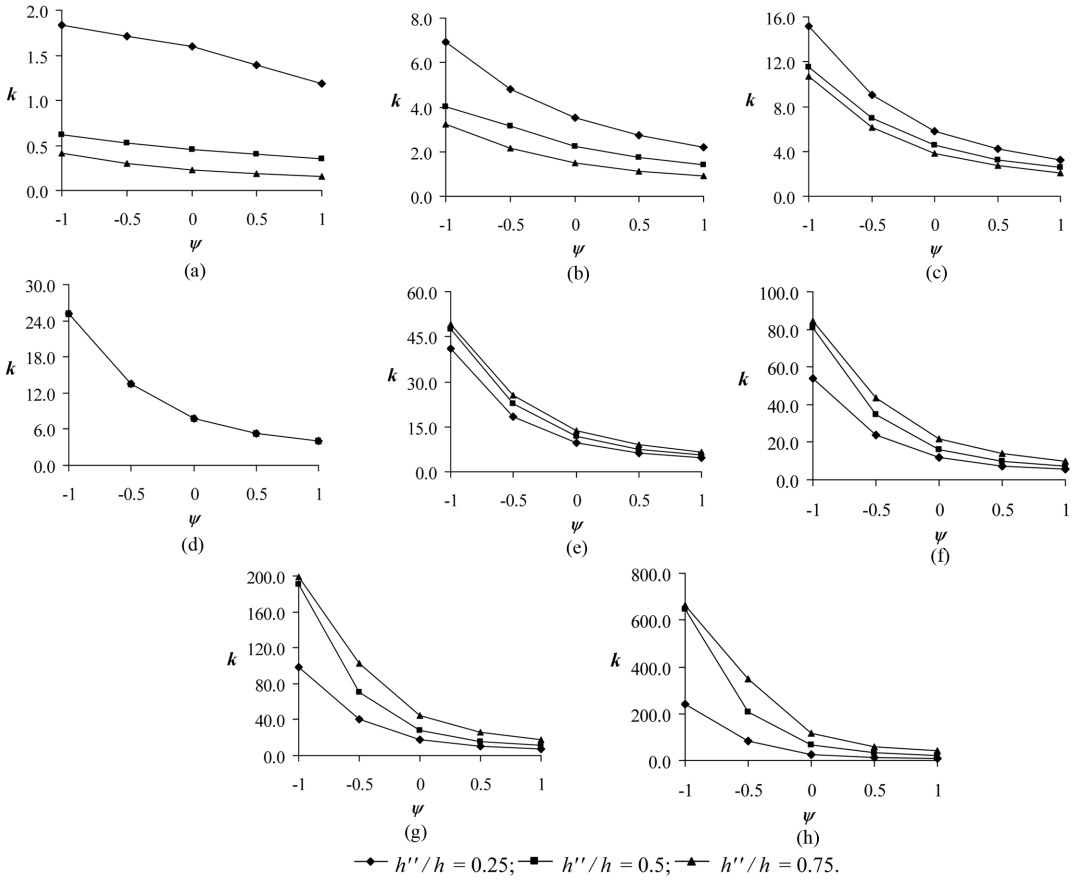

Fig. 6 Plates with $a / h = 1$. k vs. ψ diagrams for various h'' / h and t'' / t' ratios: $t'' / t' = 0.25$ (a); 0.5 (b); 0.75 (c); 1 (d); 1.25 (e); 1.5 (f); 2 (g); 3 (h)

$t''/t' = 0.5$ (Fig. 6(b)), $t''/t' = 0.75$ (Fig. 6(c)); $t''/t' = 1$ (Fig.6(d)), $t''/t' = 1.25$ (Fig. 6(e)), $t''/t' = 1.5$ (Fig. 6(f)), $t''/t' = 2$ (Fig. 6(g)) and $t''/t' = 3$ (Fig. 6(h)).

The diagrams show similar trends when load configuration varies since a reduction in k when ψ varies from -1 to 1 is observed. For $t''/t' = 0.25$ (see Fig. 6(a)), the values of k, although rather small, denote a high difference between the ratio $h''/h = 0.25$ and the ratios 0.5 and 0.75. In particular there is a strong reduction of k from $h''/h = 0.25$ to 0.5, and a small reduction from $h''/h = 0.5$ to 0.75.

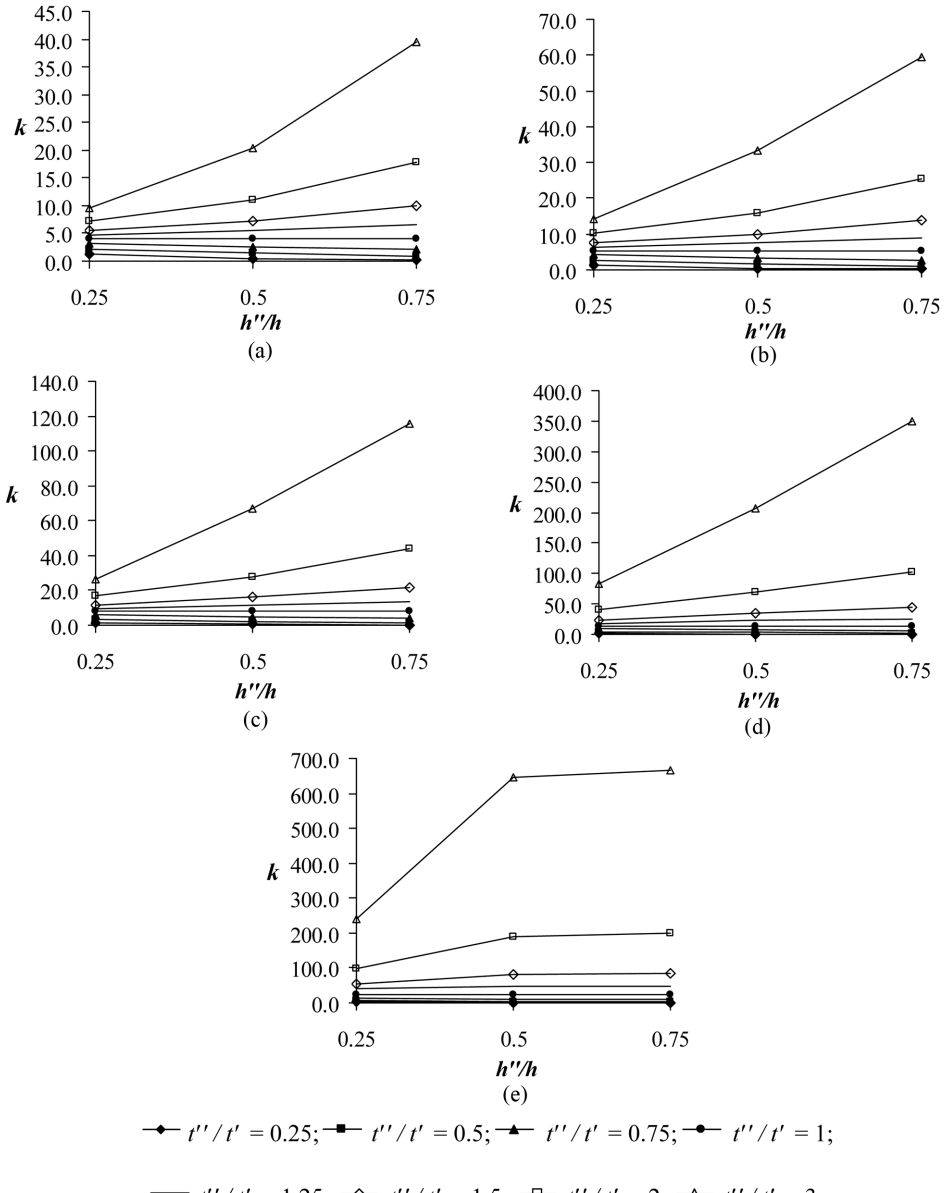

Fig. 7 Plates with $a/h = 1$. k vs. h''/h diagrams, for various t''/t' and ψ ratios: $\psi = 1$ (a); $\psi = 0.5$ (b); $\psi = 0$ (c); $\psi = -0.5$ (d); $\psi = -1$ (e)

Furthermore, for $t''/t' = 0.25$, buckling occurs with half-waves involving the deformation of the slender subpanel only.

Increasing the ratio t''/t' towards the unit (corresponding to the plate with constant thickness), the curves tend to become closer (until one curve only when $t''/t' = 1$, see Fig. 6(d)) and the deformed shape tends to involve the entire panel. When the thickness of the top subpanel becomes greater than that of the lower subpanel ($t''/t' > 1$), a reversal of position of the curves corresponding to $h''/h = 0.25$ and 0.75 happens and a significant increase in values of k occurs.

Fig. 7 shows k vs. h''/h diagrams, when t''/t' varies for various stress ratios $\psi = 1$ (Fig. 7(a)), $\psi = 0.5$ (Fig. 7(b)), $\psi = 0$ (Fig. 7(c)), $\psi = -0.5$ (Fig. 7(d)) and $\psi = -1$ (Fig. 7(e)). The trend of the curves in Fig. 7 is similar for every loading conditions. The slopes of the two parts of the bilinear curves are similar, with a significant increase in the second part between $h''/h = 0.5$ and 0.75 for $t''/t' > 1$ and a small decrease for $t''/t' = 1$. The case $t''/t' = 1$is represented by a linear function with constant slope. For $\psi = -1$, the slope decreases in the second part of the diagram ($h''/h > 0.5$).

Fig. 8 shows number of half-waves vs. t''/t' diagrams for various values of the ratio h''/h and $\psi = -1$ (Fig. 8(a)), $\psi = -0.5$ (Fig. 8(b)), $\psi = 0$ (Fig. 8(c)), $\psi = 0.5$ (Fig. 8(d)) and $\psi = 1$ (Fig. 8(e)), for plates

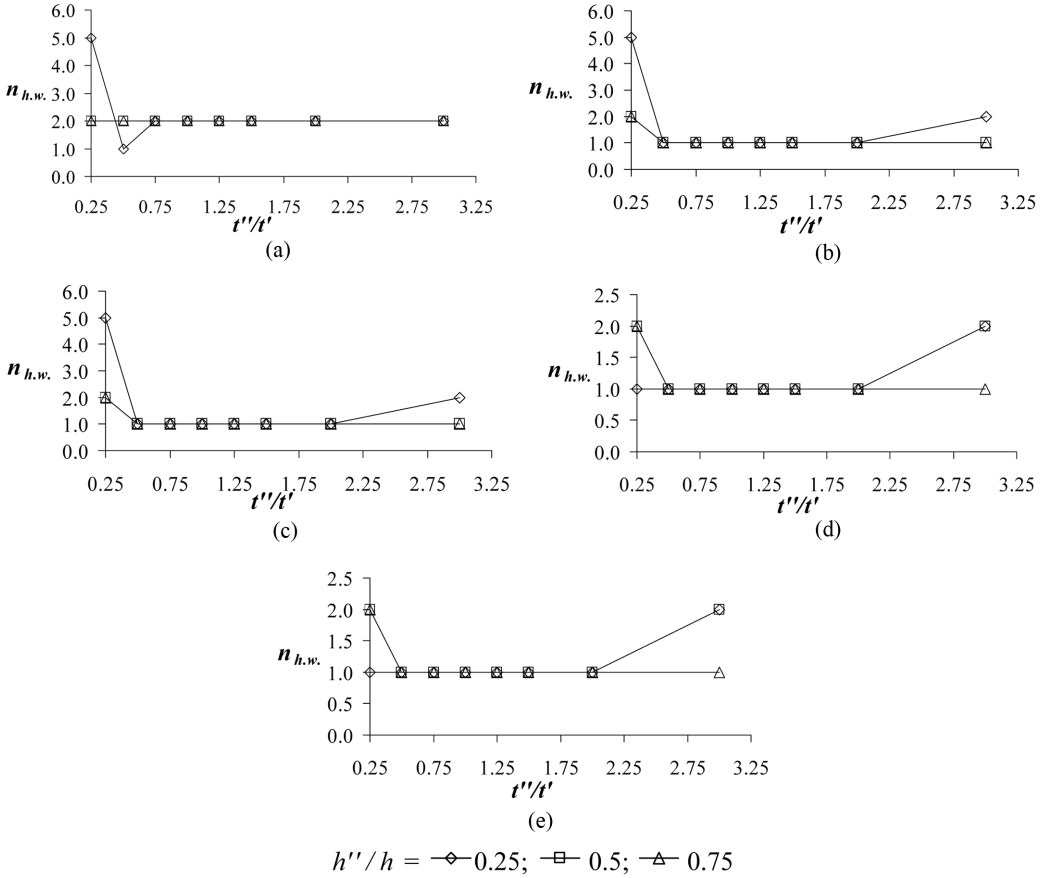

Fig. 8 Plates with $a/h = 1$. Number of half-waves vs. t''/t' diagrams for various h''/h and ψ ratios: $\psi = -1$ (a); $\psi = -0.5$ (b); $\psi = 0$ (c); $\psi = 0.5$ (d); $\psi = 1$ (e)

with $a/h = 1$. When $0.5 < t''/t' < 2$ the critical deformed shape shows one half-wave only (as for the case of constant thickness). When $t''/t' = 0.25$ and 3 the critical deformed shape strongly varies with respect to the case of constant thickness and the two subpanels show separate buckling shapes.

4. Rectangular plates

In this section, the behaviour in terms of global buckling coefficient k of rectangular plates with $a/h = 2$ and 3 formed by two subpanels subjected to various stress ratios ψ is shown and discussed when h''/h and t''/t' vary. Fig. 9 shows, for plates with $a/h = 2$, the k vs. ψ diagrams for various h''/h and ratios t''/t'=0.25 (Fig. 9(a)), $t''/t' = 0.5$ (Fig. 9(b)), $t''/t' = 0.75$ (Fig. 9(c)), $t''/t' = 1$ (Fig. 9(d)), $t''/t' = 1.25$ (Fig. 9(e)), $t''/t' = 1.5$ (Fig. 9(f)), $t''/t' = 2$ (Fig. 9(g)) and $t''/t' = 3$ (Fig. 9(h)). As for square plates (see Fig. 6), a reduction in k when ψ varies from -1 to 1 is observed. For the plates with $a/h = 2$ composed by subpanels with thickness ratio $t''/t' = 0.25$, the value of k still denotes a strong variation

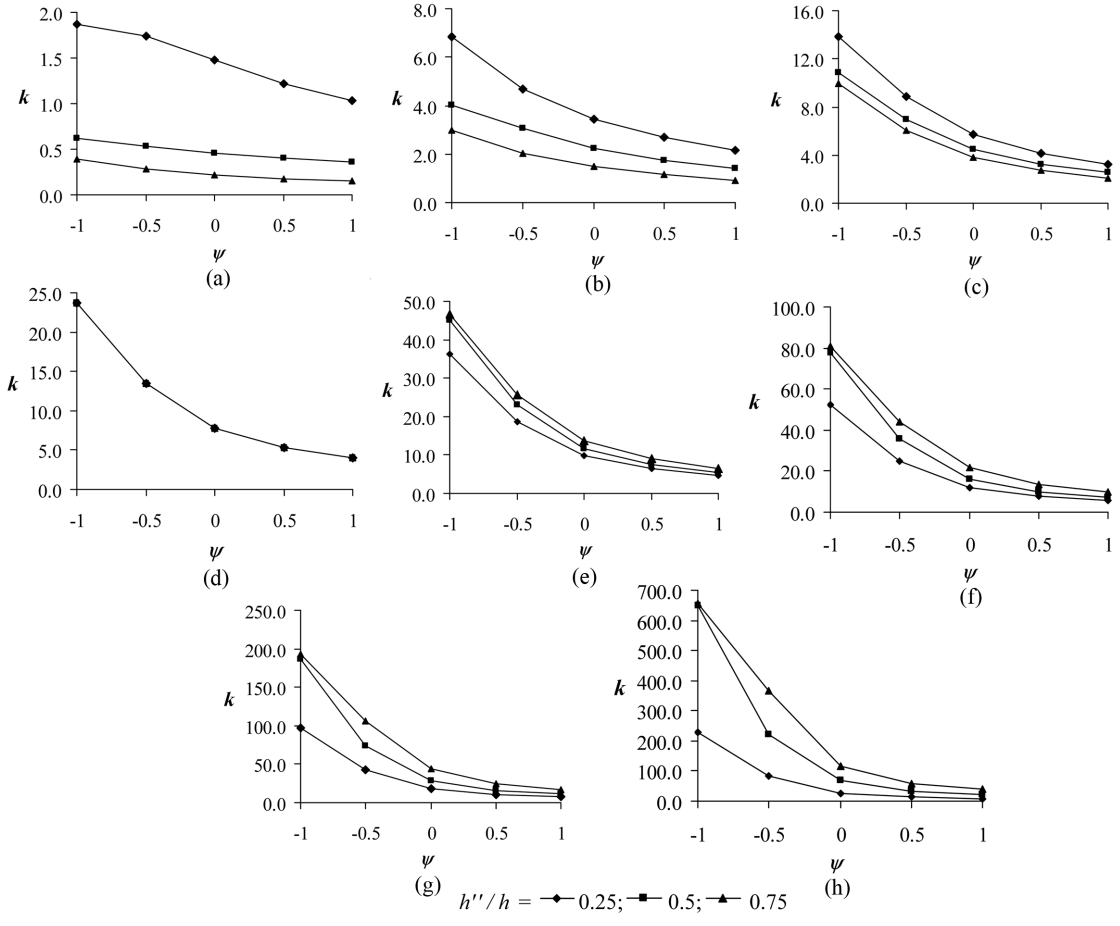

Fig. 9 Plates with $a/h = 2$. k vs. ψ diagrams for various h''/h and t''/t' ratios: $t''/t' = 0.25$ (a); 0.5 (b); 0.75 (c); 1 (d); 1.25 (e); 1.5 (f); 2 (g); 3 (h)

between the ratio $h''/h = 0.25$ and the ratios 0.5 and 0.75. Increasing the ratio t''/t' from 0.25 to 1 the curves tend again to become closer with trends similar to the case of square plates.

Fig. 10 shows k vs. h''/h diagrams, when t''/t' varies for various stress ratios $\psi = 1$ (Fig. 10a), $\psi = 0.5$ (Fig. 10(b)), $\psi = 0$ (Fig. 10(c)), $\psi = -0.5$ (Fig. 10(d)) and $\psi = -1$ (Fig. 10(e)) and Fig. 11 shows number of half-waves vs. t''/t' diagrams for various values of the ratio h''/h and $\psi = -1$ (Fig. 11(a)), $\psi = -0.5$ (Fig. 11(b)), $\psi = 0$ (Fig. 11(c)), $\psi = 0.5$ (Fig. 11(d)) and $\psi = 1$ (Fig. 11(e)). When $0.75 < t''/t' < 2$ the critical deformed shape shows, along the horizontal axis, three half waves for uniform

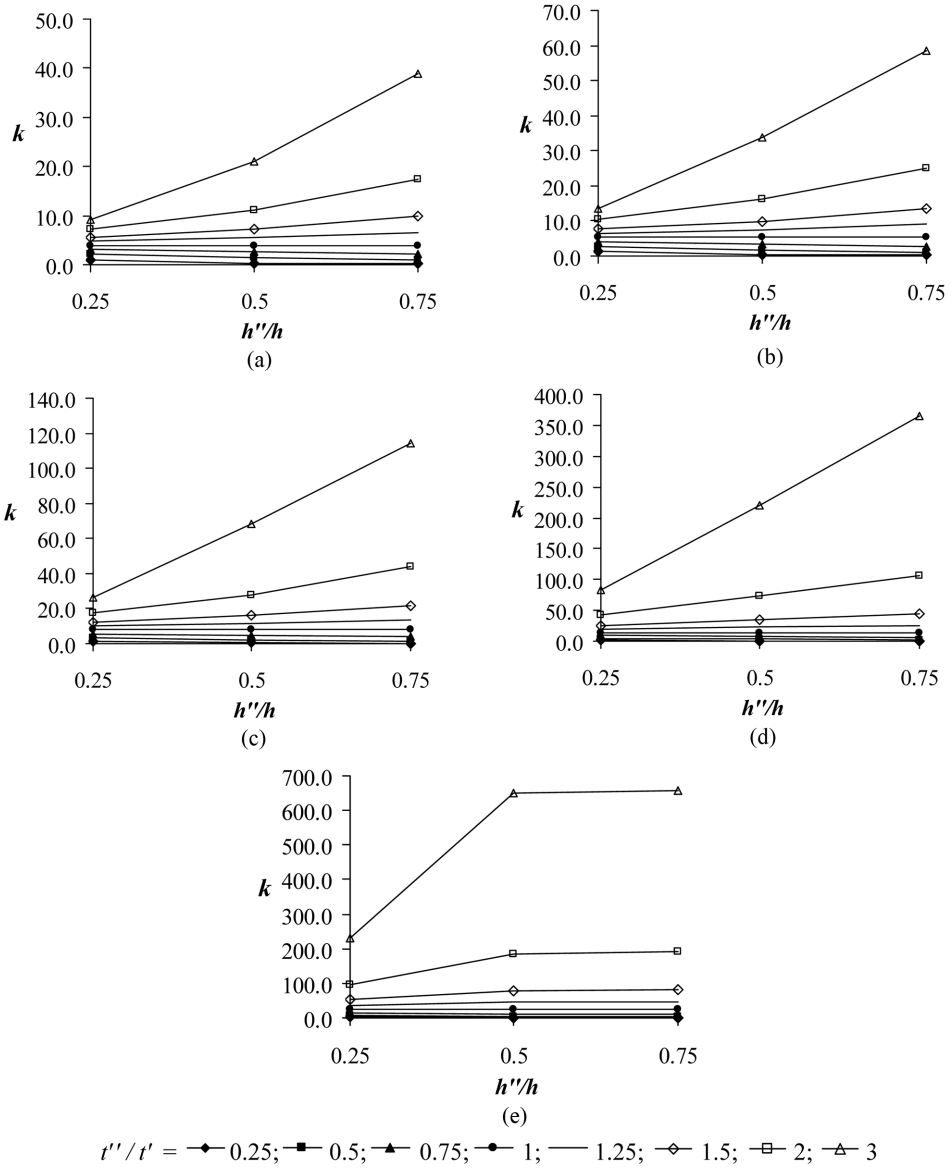

Fig. 10 Plates with $a/h = 2$. k vs. h''/h diagrams, for various t''/t' and ψ ratios: $\psi = 1$ (a); $\psi = 0.5$ (b); $\psi = 0$ (c); $\psi = -0.5$ (d); $\psi = -1$ (e)

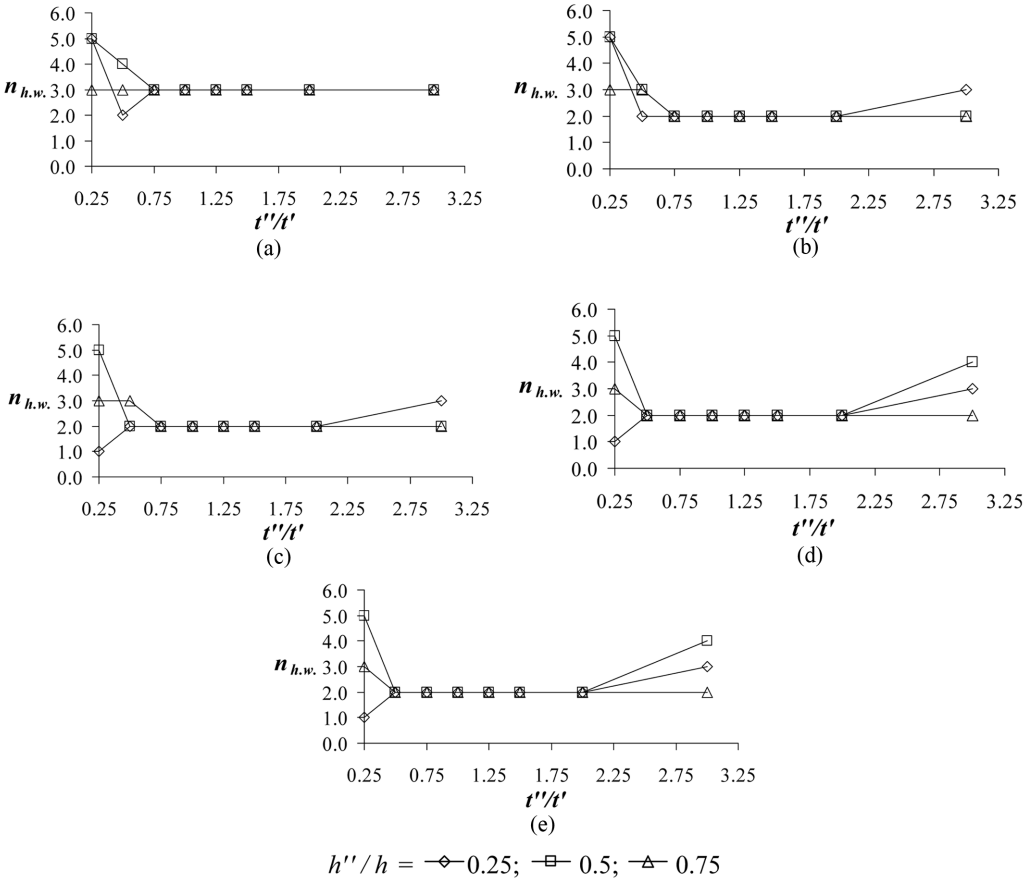

Fig. 11 Plates with a/h 2. Number of half-waves vs. t''/t' diagrams for various h''/h' and ψ ratios: $\psi = -1$ (a); $\psi = -0.5$ (b); $\psi = 0$ (c); $\psi = 0.5$ (d); $\psi = 1$ (e)

compression ($\psi = 1$) and two half-waves for the other values of ψ. When $t''/t' = 0.25$, 0.75 (in some cases) and 3 the critical deformed shape strongly varies with respect to the case of constant thickness and the two subpanels show separate buckling shapes with a different number of half-waves. The deformed shape along the vertical axis always shows one half-wave.

In Fig. 12 k vs. ψ diagrams for various values of h''/h and $t''/t' = 0.25$ (Fig. 12(a)), $t''/t' = 0.5$ (Fig. 12(b)), $t''/t' = 0.75$ (Fig. 12(c)), $t''/t' = 1$ (Fig. 12(d)), $t''/t' = 1.25$ (Fig. 12(e)), $t''/t' = 1.5$ (Fig. 12(f)), $t''/t' = 2$ (Fig. 12(g)) and $t''/t' = 3$ (Fig. 12(h)) are shown for plates having $a/h = 3$.

Fig. 13 shows, again for plates with $a/h = 3$, k vs. h''/h diagrams, when t''/t' varies for various stress ratios $\psi = 1$ (Fig. 13(a)), $\psi = 0.5$ (Fig. 13(b)), $\psi = 0$ (Fig. 13(c)), $\psi = -0.5$ (Fig. 13(d)) and $\psi = -1$ (Fig. 13(e)) and Fig. 14 shows number of half-waves vs. t''/t' diagrams for various values of the ratio h''/h and $\psi = -1$ (Fig. 14(a)), $\psi = -0.5$ (Fig. 14(b)), $\psi = 0$ (Fig. 14(c)), $\psi = 0.5$ (Fig. 14(d)) and $\psi = 1$ (Fig. 14(e)). k vs. ψ and k vs. h''/h diagrams for plates with $a/h = 3$ have similar trends to those corresponding to $a/h = 1$ and 2 with slightly different values. In the critical deformed shape of the rectangular plate with $a/h = 3$ and constant thickness the number of half-waves of the deformed shape varies according to the applied load. The plate with $a/h = 3$ and constant thickness presents a critical

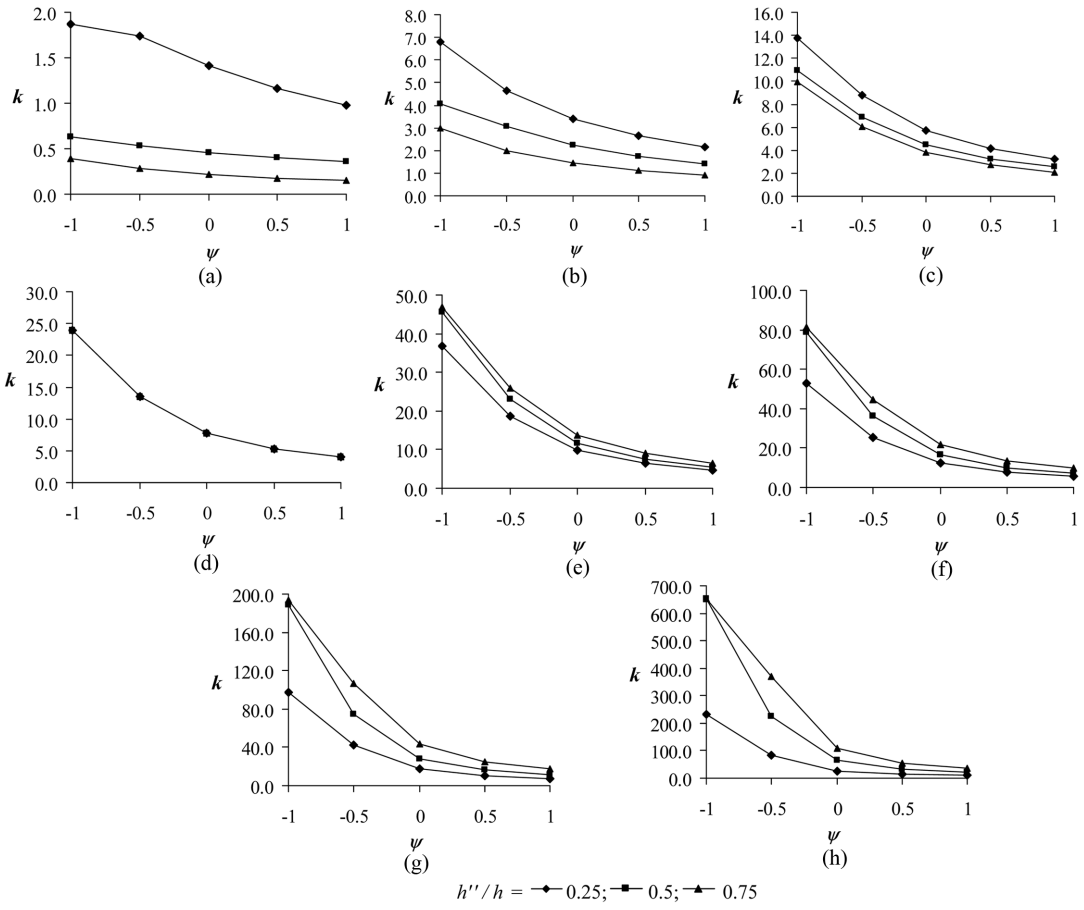

Fig. 12 Plates with $a/h = 3$. k vs. ψ diagrams for various h''/h and t''/t' ratios: $t''/t' = 0.25$ (a); 0.5 (b); 0.75 (c); 1 (d); 1.25 (e); 1.5 (f); 2 (g); 3 (h)

deformed shape with three half-waves along the horizontal direction when subjected to a uniform compression load. The same type of deformed shape occurs for the loading conditions with $\psi = 0.5$, 0 and –0.5, whereas, for $\psi = -1$, the deformed shape along the horizontal axis consists in five half-waves. When $t''/t' \neq 1$ the critical deformed shape strongly varies with respect to the case of constant thickness and the two subpanels show separate buckling shapes with a different number of half-waves. This circumstance is more evident than the case of $a/h = 2$. The deformed shape along the vertical axis always shows one half-wave with various positions of the maximum deformation.

5. Discussion and proposal of simplified design formulas

In this section specific analytical formulations are proposed for assessing k in all geometric configurations proposed. Figs. 15(a), (b) and (c) show the comparisons between all the geometric and load combinations taken into consideration in this study in terms of k vs. ψ diagrams when the ratio $t''/$

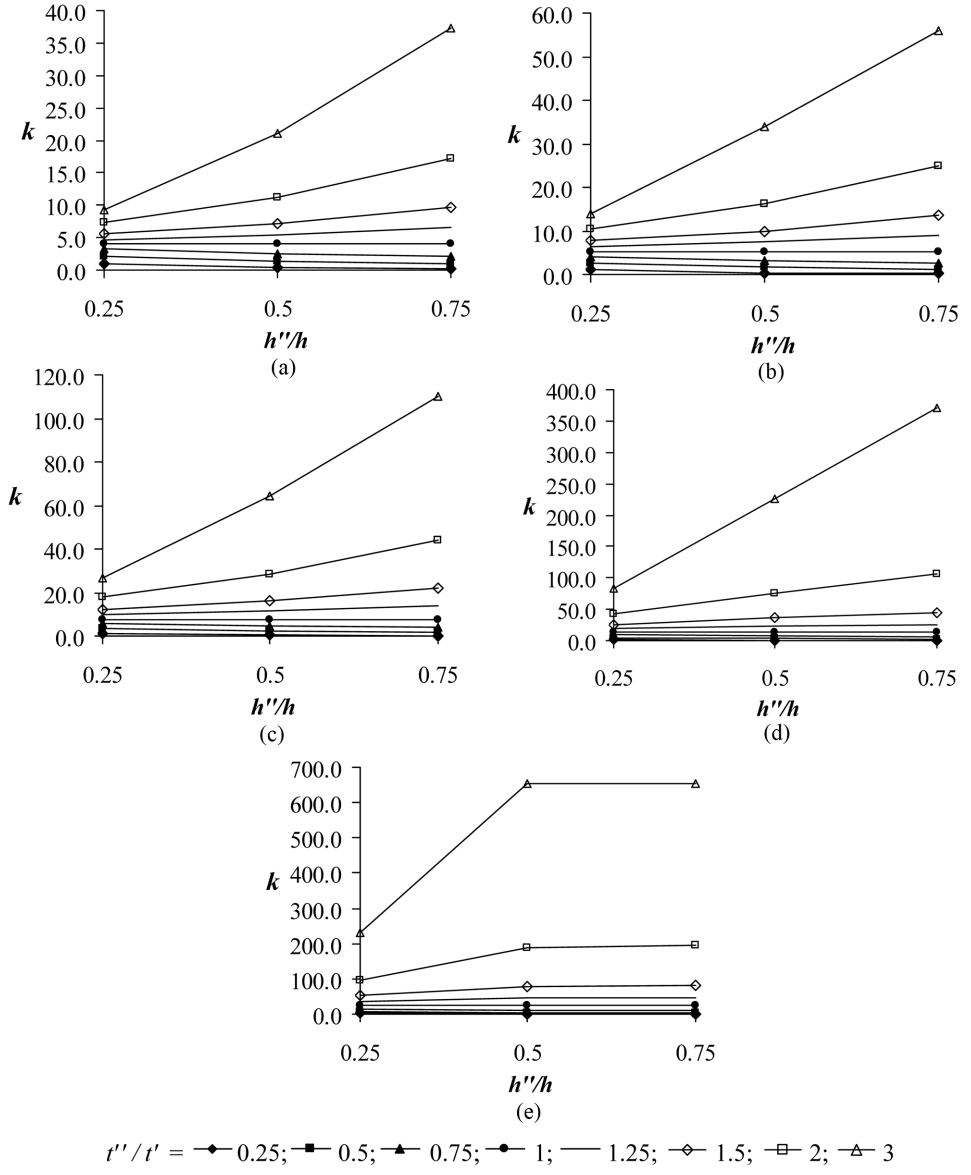

Fig. 13 Plates with $a/h = 3$. k vs. h''/h diagrams, for various t''/t' and ψ ratios: $\psi = 1$ (a); $\psi = 0.5$ (b); $\psi = 0$ (c); $\psi = -0.5$ (d); $\psi = -1$ (e)

t' varies ($h''/h = 0.25$ in Fig. 15(a), $h''/h = 0.5$ in Fig. 15(b), $h''/h = 0.75$ in Fig. 15(c)).

The values of k obtained for square plates do not substantially differ from those corresponding to rectangular plates with $a/h = 2$ and 3 for any load configuration since the plates with $a/h = 2$ and 3 can be considered as composed by two or three square subpanels respectively. This is confirmed in Timoshenko and Woinowsky-Krieger (1959) due to the multi-wave critical shape of the rectangular plates (for each square subpanel the critical deformed shape does not substantially differ).

The slope of the curves in Fig. 15 decreases moving from $\psi = -1$ to 1. An increase of k is observed

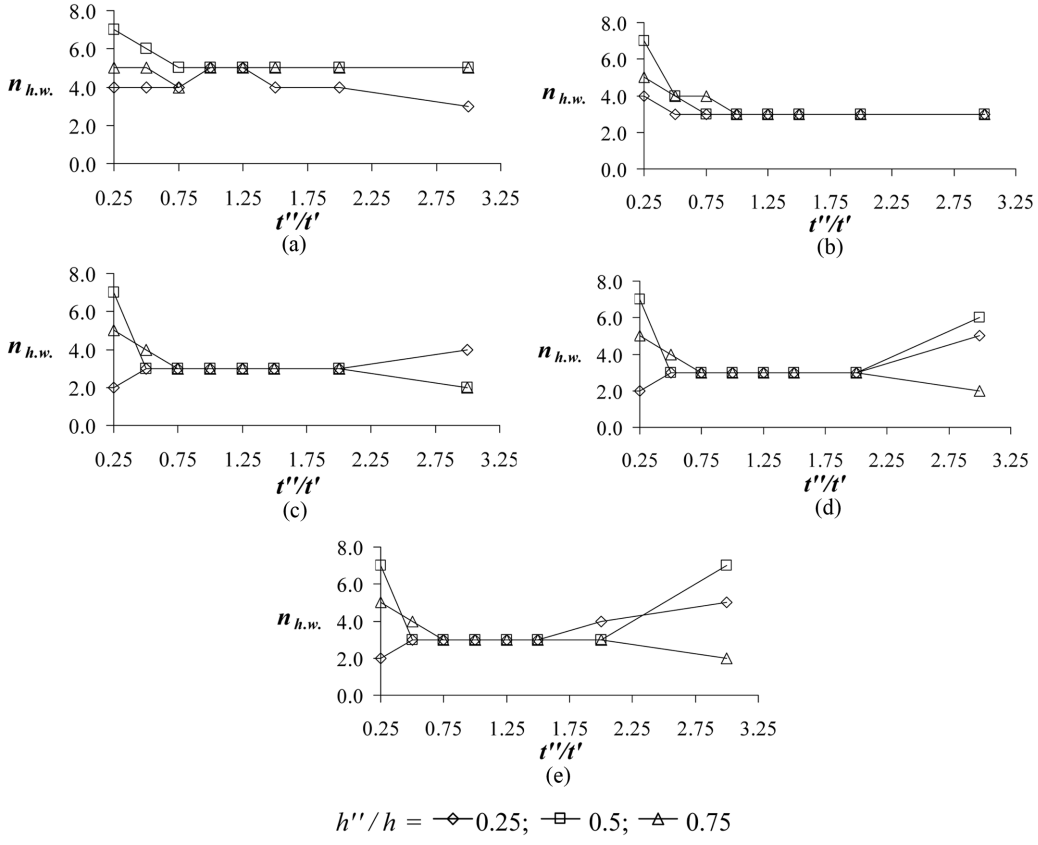

Fig. 14 Plates with $a/h = 3$. Number of half-waves vs. t''/t' diagrams for various h''/h and ψ ratios: $\psi = -1$ (a); $\psi = -0.5$ (b); $\psi = 0$ (c); $\psi = 0.5$ (d); $\psi = 1$ (e)

when moving from $h''/h = 0.25$ to 0.5, whereas k does not practically vary from $h''/h = 0.5$ to 0.75, even for high t''/t' ratios.

Table 1 shows the proposed analytical formulas for the calculation of k. The expressions for k were obtained on the basis of the numerical results of the linear buckling analyses with the aim of proposing a practical instrument for the estimation of k at the same time reliable and not too much complicated. With the exception of the first expression, all the other expressions include an incremental formula, to be added, in most cases, to the value corresponding to the panel with constant thickness.

The expressions for the buckling coefficient k in Table 1 were obtained with the following procedure. Assuming as a starting point the basic situation in which the panel has uniform thickness ($t''/t' = 1$), constant values of k (with sums of Table 1 equal to 0) were found according to code provisions (if existing for the specific case). Furthermore, according to the above numerical results, it can be observed that k increases, with various slopes, when ψ, h''/h and t''/t' increase; hence the basic idea is to use incremental formulations for predicting the buckling coefficient. In particular a constant step of 0.25 was assumed for the increments of the ratio t''/t'. The basic values related to the panel with uniform thickness were assumed as those to which the values resulting from the various sums have to be added when sub-panels have variable thicknesses. The index x of the sum is defined according to the integer

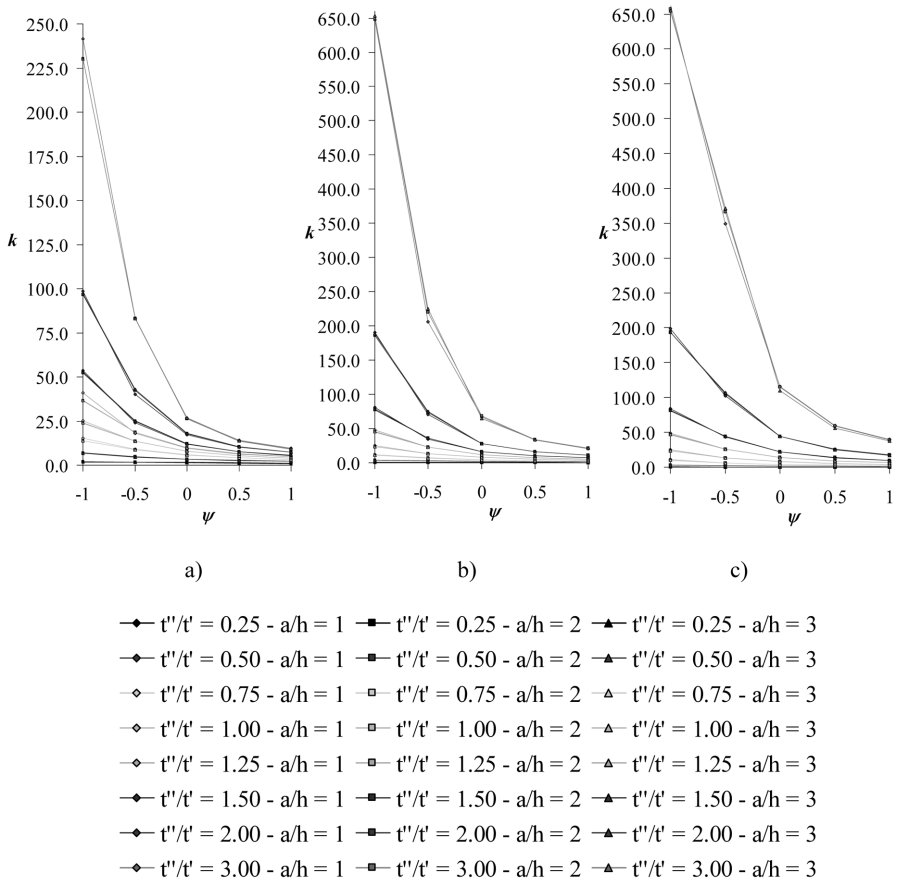

Fig. 15 k vs. ψ diagrams for various t''/t' and h''/h ratios: $h''/h = 0.25$ (a); 0.5 (b); 0.75 (c)

quantity n which depends on the ratio t''/t'. The integer quantity n is defined with the aim of obtaining the number of steps necessary to update the result of the sum. The sums were built for each case assuming as parameters ψ, h''/h and t''/t' (for $a/h = 1, 2, 3$).

This procedure, based on incremental formulations, seem to led to more accurate expressions with respect to expressions resulting from regression analyses (not easy to be developed due to the number of parameters of the problem) and, at the same time, suitable for the use in the design practice. In particular the incremental formulation allows to reduce the number of expressions when t''/t' varies.

For example, for $h''/h = 0.5$, $t''/t' = 1.5$ and $\psi = -1$ it is obtained

$$n = \frac{(t''/t') - 1}{0.25} = 2 \tag{8}$$

$$k = 23.9 + \sum_{x=0}^{n-1} (22.1 + 11.1x) = 23.9 + 22.1 + 11.1 \times 0 + 22.1 + 11.1 \times 1 = 79.2 \tag{9}$$

In Table 2 a comparison between the results derived by the proposed equations and corresponding

Table 1 Proposed design formulas for k in panels with variable thickness (t''/t') variable with intervals equal to 0.25).

ψ	h''/h	k	n	t''/t'
1	0.25	$4 + 2.8\left(\frac{t''}{t'} - 1\right)$		
	0.50	$0.4 + \sum_{x=0}^{n-1}(1 + 0.2x)$	$\frac{(t''/t') - 0.25}{0.25}$	≥ 0.25
	0.75	$0.1 + \sum_{x=0}^{n}(0.65x)$		
0.5	0.25	$5.25 + \sum_{x=0}^{n-1}(1.1 + 0.1x)$ $5.25 - \sum_{x=0}^{n-1}(1.1 + 0.1x)$	$\frac{(t''/t') - 1}{0.25}$	≥ 1 < 1
	0.50	$0.35 + \sum_{x=0}^{n-1}(1.3 + 0.35x)$	$\frac{(t''/t') - 0.25}{0.25}$	≥ 0.25
	0.75	$0.2 + \sum_{x=0}^{n-1}(0.7 + x)$		
0	0.25	$7.64 + 8\left(\frac{t''}{t'} - 1\right)$		
	0.50	$1.3 + \sum_{x=0}^{n-1}(1.1 + x)$	$\frac{(t''/t') - 0.25}{0.25}$	≥ 0.25
	0.75	$0.85 + \sum_{x=0}^{n-1}(0.65 + 1.6x)$		
−0.5	0.25	$2.628 + \sum_{x=0}^{n-1}(2.55 + x)$		
	0.50	$7.068 + \sum_{x=0}^{n}(6.2 + 3.6x)$	$\frac{(t''/t') - 1}{0.25}$	≥ 1
		$7.068 - \sum_{x=0}^{n}(4 - 1.5x)$	$\frac{0.5 - (t''/t')}{0.25}$	≤ 0.5
	0.75	$5.968 + \sum_{x=0}^{n}(7.3 + 5.3x)$	$\frac{(t''/t') - 1}{0.25}$	≥ 1
		$5.968 - \sum_{x=0}^{n}(4 - 2.5x)$	$\frac{0.5 - (t''/t')}{0.25}$	≤ 0.5

Table 1 Continued

ψ	h''/h	k	n	t''/t'
−1	0.25	$1.7 + \sum_{x=0}^{n-1} (4.6 + 2.8x)$	$\frac{(t''/t') - 0.25}{0.25}$	≥ 0.25
	0.50	$23.9 + \sum_{x=0}^{n-1} (22.1 + 11.1x)$	$\frac{(t''/t') - 1}{0.25}$	≥ 1
		$10.9 + \sum_{x=0}^{n} (7 - 4x)$	$\frac{0.5 - (t''/t')}{0.25}$	≤ 0.5
	0.75	$9.9 + \sum_{x=0}^{n} (14 + 10x)$	$\frac{(t''/t') - 1}{0.25}$	≥ 1
		$9.9 - \sum_{x=0}^{n} (7 - 5x)$	$\frac{0.5 - (t''/t')}{0.25}$	≤ 0.5

numerical analyses is shown to assess the validity of the proposed equations. A general agreement between the values of the buckling coefficient obtained with the proposed equations and those provided by the numerical analyses can be observed. Proposed formulations generally tend conservatively to remain below the values obtained by the numerical analyses.

6. Conclusions

This work investigated the buckling behaviour of panels with different thicknesses subjected to both in-plane axial compression and bending moment. The variables considered for this study were the following:

- aspect ratio: $a / h = 1$, 2 and 3 (square and rectangular panels);
- stress ratio: $\psi = -1$, –0.5, 0, 0.5, and 1;
- ratio between the heights of the two subpanels: $h'' / h = 0.25$, 0.5 and 0.75;
- ratio between the thicknesses of the two subpanels: $t'' / t' = 0.25$, 0.5, 0.75, 1, 1.25, 1.5, 2 and 3.

Critical deformed shapes generated by the different types of applied load were numerically observed and compared for a number of combinations of the above variables. Curves describing the variation of the buckling coefficient k with stress ratio ψ, ratio between the thicknesses of the subpanels t'' / t' and ratio between the heights of the two subpanels h'' / h were provided.

Since, at the moment, practical expression for predicting the buckling coefficient k for welded girder webs with variable thickness subjected to axial force and bending moment are not included in the current codes, simple analytical design formulas for the estimation of k were proposed for the geometrical and load situations derived by the combinations of the above variables. The values of k obtained with the proposed analytical formulas are generally in agreement and, in most cases, conservative when compared with the values of k obtained with the specific numerical analyses. An example showing the practical use of the proposed methodology was shown.

Table 2 Comparison between buckling coefficients derived by the proposed equations and corresponding numerical analyses (Numerical Analysis = NA; Proposed Method = PM).

Values of k with $a/h = 1$ and $h''/h = 0.25$										
	$\psi = -1$		$\psi = -0.5$		$\psi = 0$		$\psi = 0.5$		$\psi = 1$	
t''/t'	NA	PM	NA	PM	NA	PM	NA	PM	NA	PM
0.25	1.8	1.7	1.7	2.6	1.6	1.6	1.4	1.7	1.2	1.9
0.50	6.9	6.3	4.8	5.2	3.5	3.6	2.7	3.0	2.2	2.6
0.75	15.1	13.7	9.0	8.7	5.8	5.6	4.2	4.2	3.2	3.3
1.00	25.2	23.9	13.5	13.3	7.8	7.6	5.3	5.3	4.0	4.0
1.25	41.0	36.9	18.2	18.8	9.7	9.6	6.3	6.4	4.7	4.7
1.50	53.6	52.7	23.9	25.4	11.8	11.6	7.5	7.6	5.5	5.4
2.00	98.7	92.7	40.2	41.5	17.2	15.6	10.3	10.3	7.2	6.8
3.00	241.6	206.3	83.3	85.7	26.6	23.6	14.1	16.9	9.5	9.6
Values of k with $a/h = 2$ and $h''/h = 0.5$										
	$\psi = -1$		$\psi = -0.5$		$\psi = 0$		$\psi = 0.5$		$\psi = 1$	
t''/t'	NA	PM	NA	PM	NA	PM	NA	PM	NA	PM
0.25	0.6	0.9	0.5	0.6	0.5	1.3	0.4	0.4	0.4	0.4
0.50	4.0	3.9	3.1	3.1	2.2	2.4	1.7	1.7	1.4	1.4
0.75	10.9	10.9	6.9	7.1	4.5	4.5	3.3	3.3	2.5	2.6
1.00	23.7	23.9	13.5	13.3	7.8	7.6	5.3	5.3	4.0	4.0
1.25	45.0	46.0	23.0	23.1	11.7	11.7	7.5	7.7	5.5	5.6
1.50	77.5	79.2	35.7	36.5	16.3	16.8	10.0	10.4	7.1	7.4
2.00	185.9	178.9	73.6	74.1	28.0	30.0	16.1	16.8	11.2	11.6
3.00	649.1	511.5	220.1	192.5	68.2	68.4	33.9	33.9	21.0	22.4
Values of k with $a/h = 3$ and $h''/h = 0.75$										
	$\psi = -1$		$\psi = -0.5$		$\psi = 0$		$\psi = 0.5$		$\psi = 1$	
t''/t'	NA	PM	NA	PM	NA	PM	NA	PM	NA	PM
0.25	0.4	0.9	0.3	0.5	0.2	0.9	0.2	0.2	0.2	0.1
0.50	3.0	2.9	2.0	2.0	1.5	1.5	1.1	0.9	0.9	0.8
0.75	10.0	9.9	6.0	6.0	3.8	3.8	2.7	2.6	2.1	2.1
1.00	23.9	23.9	13.5	13.3	7.8	7.6	5.3	5.3	4.0	4.0
1.25	46.9	47.9	25.8	25.9	13.8	13.1	9.0	9.0	6.6	6.6
1.50	81.5	81.9	44.5	43.8	21.8	20.1	13.6	13.7	9.7	9.9
2.00	193.9	179.9	106.6	95.5	43.9	39.0	25.0	26.1	17.3	18.3
3.00	654.7	495.9	370.9	262.5	109.9	96.0	55.9	62.9	37.2	43.0

Acknowledgements

The writers wish to thank Mr S.Gugole for the contribution to some numerical analyses developed during the thesis (Gugole 2009).

References

Alinia, M. M. (2005), "A study into optimization of stiffeners in plates subjected to shear loading", *Thin-Walled Structures*, **43**(5), 845-860.

Alinia, M. M. and Dastfan, M. (2006), "Behaviour of thin steel plate shear walls regarding frame members", *Journal of Constructional Steel Research*, **62**(7), 730-738.

Azhari, M., Shahidi, A.R. and Saadatpour, M.M. (2005), "Local and post local buckling of stepped and perforated thin plates", *Applied Mathematical Models*, **29**(7), 633-652.

Chatterjee, S. (2003) The Design of Modern Steel Bridges, 2nd ed., ISBN: 0632055111, Wiley-Blackwell.

Cheng, C. J. and Fan, X.J. (2001), "Nonlinear mathematical theory of perforated viscoelastic thin plates with its applications", *International Journal of Solids and Structures*, **38**(36), 6627-6641.

El-Sawy, K. M., Nazmy, A. S. and Mohammad, I. M. (2004), "Elasto plastic buckling of perforated plates under uniaxial compression", *Thin-Walled Structures*, **42**(8), 1083-1101.

El-Sawy, K.M. and Ikbal Martini, M. (2007), "Elastic stability of bi-axially loaded rectangular plates with a single circular hole", *Thin-Walled Structures*, **45**(1), 122-133.

EN 1993-1-5 (2007), "Eurocode 3. Design of steel structures. Part 1-5: Stiffened plating subjected to in plane loading", CEN European Committee for Standardization, Brussels.

G. D Computing (2005), Straus7 user's manual, Sydney, Australia.

Graciano, C. and Casanova, E. (2005), "Ultimate strength of longitudinally stiffened I-girder webs subjected to combined patch loading and bending", *Journal of Constructional Steel Research*, **61**(1), 93-111.

Granath, P. and Lagerqvist, O. (1999), "Behaviour of girder webs subjected to patch loading", *Journal of Constructional Steel Research*, **50**(1), 49-69.

Gugole, S. (2009), "Stabilità di pannelli d'anima con spessore variabile" (in italian), Master thesis, University of Padova.

Komur, M.A. and Sonmez. M. (2008), "Elastic buckling of rectangular plates under linearly varying in-plane normal load with a circular cutout", *Mechanics Research Communications*, **35**, 361-371.

Lee, S.C., Yoo, C.H. and Yoon D.Y. (2002), "Behaviour of intermediate transverse stiffeners attached on web panels", Journal of Structural Engineering, *Transactions of ASCE* **128**(3), 337-345.

Lian, V.T. and Shanmugam N.E. (2003), "Openings in horizontally curved plate girder webs", *Thin-Walled Structures*, **41**(2-3), 245-269.

Maiorana, E., Pellegrino, C. and Modena, C. (2008a), "Linear buckling analysis of unstiffened plates subjected to both patch load and bending moment", *Engineering Structures* **30**(12), 3731-3738.

Maiorana, E., Pellegrino, C. and Modena, C. (2008b), "Linear buckling analysis of perforated plates subjected to localised symmetrical load", *Engineering Structures* **30**(11), 3151-3158.

Maiorana, E., Pellegrino, C. and Modena, C. (2009a), "Imperfections in steel girder webs with and without perforations under patch loading", *Journal of Constructional Steel Research*, **65**(5), 1121-1129.

Maiorana, E., Pellegrino, C., and Modena, C. (2009b), "Elastic stability of plates with circular and rectangular holes subjected to axial compression and bending moment", *Thin-Walled Structures*, **47**(3), 241-255.

Maiorana, E., Pellegrino, C., and Modena, C. (2009c), "Non-Linear analysis of perforated steel plates subjected to localised symmetrical load", *Journal of Constructional Steel Research*, **65**(4), 959-964.

Maiorana E., Pellegrino C., Modena C. (2011a), "Influence of longitudinal stiffeners on elastic stability of girder webs", *Journal of Constructional Steel Research*, **67**(1), 51-64.

Maiorana E., Pellegrino C., Modena C. (2011b), "Elasto-plastic behaviour of perforated steel plates subjected to compression and bending", *Steel and Composite Structures*, **11**(2), 131-147.

Maryland, T., Hopperstad, O.S. and Langseth, M. (1999), "Steel girders subjected to concentrated loading. Validation of numerical simulations", *Journal of Constructional Steel Research*, **50**, 199-216.

Paik, J.K. (2007), "Ultimate strength of perforated steel plates under shear loading", *Thin-Walled Structures*, **45**(3), 301–306.

Pavlovčič, L., Detzel, A., Kuhlmann, U. and Beg, D. (2007), "Shear strength of longitudinally stiffened panels. Part 1: Tests and numerical analysis of imperfections", *Journal of Constructional Steel Research*, **63**(3), 337-350.

Pellegrino, C., Maiorana, E. and Modena, C. (2009), "Linear and non-Linear behaviour of perforated steel plates

with circular and rectangular holes under shear loading", *Thin-Walled Structures*, **47**(6-7), 607-616.
Ren, T. and Tong, G.S. (2005), "Elastic buckling of web plates in I-girders under patch and wheel loading", *Engineering Structures*, **27**(10), 1528-1536.
Sadovský, Z., Teixeria, A.P. and Guedes Soares, C. (2005), "Degradation of the compressive strength rectangular plates due to initial deflection", *Thin-Walled Structures*, **43**(1), 65-82.
Timoshenko, S.P. and Woinowsky-Krieger, S. (1959), Theory of plates and shells, Mc-Graw-Hill Book Company.
Xie, M. and Chapman, J.C. (2004), "Design of web stiffeners: local panel bending effects", *Journal of Constructional Steel Research*, **60**(10), 1425-1452.
Yang, Z., Kim, C., Cho, C. and Beom, H.G. (2008), "The concentration of stress and strain in finite thickness elastic plates containing a circular hole", *International Journal of Solids and Structures*, **45**(3-4), 713-731.

CC

Appendix 1: Notation.

Symbol	Description
a	panel length
D	flexural rigidity
E	elastic modulus
h	panel's height
h'	lower sub-plate height
h''	upper sub-plate height
k	buckling coefficient
m	number of half-wave in x-dir
n	number of half-wave in y-dir
N_x	force in x-dir.
t'	lower sub-plate thickness
t''	upper sub-plate thickness
x	horizontal axis
y	vertical axis
λ	plate slenderness
ψ	stress ratio
ν	Poisson's ratio
ω	half-wave